Neuroendocrinology Letters Volume 34 No. 5 2013

ORIGINAL ARTICLE

Nitrosative-induced posttranslational α-tubulin changes on high-glucose-exposed Schwannoma cell line

Sergio Domenico Gadau

Department of Veterinary Medicine, University of Sassari, Via Vienna 2, Sassari, Italy

Correspondence to: Dr. Sergio Gadau
Department of Veterinary Medicine, University of Sassari,
Via Vienna 2, 07100, Sassari, Italy.
TEL: +39 079229596; FAX: +39 079229432; E-MAIL: sgadau@uniss.it

Submitted: 2013-03-02 Accepted: 2013-07-31 Published online: 2013-08-03

Key words: **oxidative stress; α-tubulin PTMs; 3-nitro-L-tyrosine; high D-glucose; Schwannoma cells**

Neuroendocrinol Lett 2013; **34**(5):372–382 **PMID:** 23922044 NEL340513A04

Abstract

OBJECTIVE: One of the major complications during prolonged hyperglycemic condition is the onset of the so-called diabetic neuropathy, that can affect the peripheral nervous system. Evidence has reported that glucose-induced oxidative stress could be a key mediator in this process, impairing the cytoskeletal structures, such as microtubules. In general, much attention is paid to the possible nitrosative-induced changes of neurons during hyperglycemic conditions, while little is known of the Schwann cells.

METHODS: Using morphological examination, immunofluorescence staining and western blot analysis, the possible hyperglycemic oxidative-induced microtubular changes in the RT4 Schwannoma cell line was investigated.

RESULTS: After 72 hrs of 180 mM D-glucose exposure, a decrease of total, tyrosinated and detyrosinated α-tubulins was found, whereas a significant increase of the acetylated α-tubulin isotype and 3-nitro-L-tyrosine was present, both through western blot and immunofluorescence staining. Moreover a downregulation of catalase and deacetylase Sirt2 enzymes was detected.

CONCLUSION: Our data underline the importance of nitrosative-induced microtubular alterations in the PNS, during hyperglycemic conditions, highlighting that Schwann cells may be directly involved in the pathogenesis of diabetic neuropathy, through the impairment of their microtubular network.

INTRODUCTION

Disorders of the nervous system may be accompanied by cellular, biochemical and functional abnormalities in the brain, spinal cord, or in the nerves. In the peripheral nervous system, a neuropathy indicates the damage to nerves, which may be caused, either by trauma to the nerve or the side-effects of systemic illness, such as hyperglycemia (Yasuda *et al.* 2003). Although several mechanisms underlie the pathogenesis of diabetic neuropathy, studies show that glucose-induced oxidative stress might be a key mediator in this process (Pennathur *et al.* 2004; Feldman 2003; Brownlee 2001). Oxidative stress results from an imbalance between reactive/nitrosative oxygen species (ROS/RNS) generation and antioxidant defenses (Melo *et al.* 2011; Sayre *et al.* 2008). Among ROS/RNS there are several intermediates such as nitric oxide, peroxynitrite, and hydroxyl radicals, all associated with a wide range of pathological conditions. Cells are usually provided with a variety of endogenous protective systems (e.g. catalase, glutathione, superoxide dismutase, etc.) to compensate for the potentially dangerous ROS and RNS (Halliwell 2006; Finkel 2003; Halliwell 2001). In cases where these defence mechanisms are inadequate, the cell will become dysfunctional or die. The hyperglycemic condition may be considered a potent initiator of apoptosis (Delaney *et al.* 2001) due to the excessive production of ROS with the formation of peroxynitrite and subsequent damage of cellular proteins, membrane lipids, nucleic acids and eventually cell death. One of the early events in cell injury, caused by oxidative stress, is the impairment of cytoskeletal structures such as microtubules (Allani *et al.* 2004; Bellomo & Mirabelli 1992; Rogers *et al.* 1989). Microtubules (MTs) are dynamically assembled polymers of α and β tubulin heterodimers, involved in different cellular functions such as cell mitosis, cell migration, cell motility, intracellular transport, secretion, cell shape maintenance and polarization. Tubulin, especially the α, undergoes several posttranslational modifications (PTMs) including acetylation, tyrosination, detyrosination, polyglutamylation and Delta 2modification (Wloga & Gaertig 2010; Janke & Kneussel 2010; Fukushima *et al.* 2009; Hammond *et al.* 2008; Westermann & Weber 2003). These modifications are regulated by the involvement of specific enzymes, such as tubulin tyrosine ligase (TTL), carboxipeptidase (CCP1), acetylase (MEC-17) and deacetylase (HDAC6, Sirt2) (Akella *et al.* 2010; Wade 2009; Boyault *et al.* 2007; Dompierre *et al.* 2007; Ersfeld *et al.* 1993). Among these so-called physiological PTMS, there are other modifications that could affect tubulin, with subsequent detrimental effects. Indeed, during oxidative stress conditions, peroxynitrite can react with tyrosine to form 3-nitro-L-tyrosine. This end product, considered a footprint for peroxynitrite mediated damage (Therond 2006; Sarchielli *et al.* 2003), may impair cellular structures such as microtubules, with an irreversible block of their characteristic dynamics (Chang *et al.* 2002; Eiserich *et al.* 1999). The detrimental action performed by the incorporation of 3-nitro-L-tyrosine appears to be responsible for morphological changes, cell death and subsequent onset of neurodegenerative diseases (Blanchard-Fillion *et al.* 2006). Accumulation of 3-nitro-L-tyrosine has been reported in tissues of diabetic mice, rats and humans (Drel *et al.* 2006; Pacher *et al.* 2005; Ishii *et al.* 2001; Thuraisingham *et al.* 2000). Moreover, increased 3-nitro-L-tyrosine immunoreactivity has been demonstrated in the peripheral nervous system (Cheng & Zochodne 2003) during experimental diabetic conditions.

When considering the interaction between axons and Schwann cells, it is evident that Schwann cells may play a crucial role in the pathogenesis of metabolic neuropathies (Lehmann & Hoke 2010). Since little is known about any oxidative/nitrosative-modifications on the microtubular network of Schwann cells under hyperglycemic conditions, the purpose of this work was to look further into these aspects, since, for many authors, Schwann cells are considered resistant to oxidative stress injury (Vincent *et al.* 2009; Baynes & Thorpe 1999).

MATERIALS AND METHODS

Cell culture

Undifferentiated RT4-D6P2T rat schwannoma cells were purchased from the American Type Culture Collection (Rockville, MD, USA). RT4-D6P2T cells showed distinct Schwann cell phenonotypes, such as the spindle-shaped morphology and the expression of glial cell markers (e.g., S-100 and GFAP) (Figure 1). We have been chosen a continuous cell line due to the fact that in comparison with primary Schwann cell cultures, Schwannoma cells may ensure a high number of cells, absence of connective cells, a good capability of attachment to the substratum and they display the same phenotypic and molecular features of primary Schwann cells (Hattangady *et al.* 2009; Hai *et al.* 2002).

Cells were grown in phenol-red-free RPMI-1640 medium supplemented with 10% heat-inactivated newborn calf serum, 2 mM L-glutamine, 100 units/ml penicillin G and 100 μg/ml streptomycin sulfate. Cells were incubated for 72 hours at 37 °C in a 5% CO_2 humidified atmosphere in the presence of 180 mM D-glucose (Gluc cells) or in basal conditions, control cells (in the figures namely Ctrl). Regarding the glucose dose employed, a dose-response curve was performed for the cell line (Gadau 2012). In rat schwannoma cells, the first morphological signs of significant cell suffering (proliferation rate and morphological changes) were appreciable only at 180 mM D-glucose. Up to that dose there was a normal growth rate without any significant morphological alteration. Hence, the results and pictures related to RT4-D6P2T cells presented in this paper deal with 180 mM D-glucose.

Proliferation assay

In order to better underline possible differences in the growth rate trend between control and Gluc cells, a proliferation assay was performed, scheduled at 24, 48 and 72 hours from the seeding. Cells were plated in 96-well dishes and cell proliferation was assessed using the 3-(4,5-dimethylthiazol-2-thiazolyl)-2,5-diphenyltetrazolium bromide (MTT) assay (5 mg/ml, MTT, Cell Titer 96, Promega, Madison, WI, USA). The medium was removed and the wells were washed with PBS. The 3-(4,5-dimethylthiazol-2-thiazolyl)-2,5-diphenyltetrazolium bromide (MTT) assay was performed by adding 20µl of MTT to each well. The plate was mixed and then incubated for 1hr at 37 °C. following the manufacturer's instructions. MTT [3-(4, 5-methylthiazol-2-yl)-2,5-diphenyltetrazolium bromide] colorimetric assay was employed to measure reduction of MTT dyes (tetrazolium) into formazan by mitochondrial enzymes in viable cells. Absorbance was measured setting the automatic microtiter reader at 492 nm (Shimadzu UV-1700, Pharma Spec, Japan) in the presence of an appropriate blank (without cells). All values are means of five experiments on 96-well dishes.

Western blot

After incubation with each experimental medium for 72 hours, cells were scraped and sonicated. Cells were then lysed by using a TO buffer (5mM TRIS HCl, 2 mM EGTA, 0.1 mM phenyl-methyl-sulfonyl fluoride, pH 8.0), supplemented with protease inhibitors (Complete-mini, Roche, Basel, Switzerland). Protein content was determined (DC Protein Assay, BioRad, CA, USA) and equal amounts of proteins (60 µg) were electrophoresed on 10% SDS-PAGE and transferred onto nitrocellulose membranes. Membranes were incubated overnight at 4 °C with primary antibodies against total α-tubulin (monoclonal, clone DM1A, 1:1,000, Sigma, St. Louis, MO, USA), tyrosinated α-tubulin (monoclonal, clone TUB-1A2, 1:1,000, Sigma, St. Louis, MO, USA), detyrosinated α-tubulin (polyclonal, 1:1,000, Chemicon-Millipore, USA), acetylated α-tubulin (monoclonal, clone 6-11B-1, 1:1,000, Sigma, St. Louis, MO, USA), 3-nitro-L-tyrosine (polyclonal, 1:500, Sigma, St. Louis, MO, USA), GFAP (monoclonal, clone G-A-5, 1:500, Sigma, St. Louis, MO, USA), actin (monoclonal, clone AC-40, 1:1,000, Sigma, St. Louis, MO, USA), anti-catalase (monoclonal, clone CAT-505, 1:1000, Sigma, St. Louis, MO, USA), anti-Sirt2 (polyclonal, 1:1000, Sigma, St. Louis, MO, USA) and anti β-Actin (monoclonal, clone AC-15, 1:1000, Sigma, St. Louis, MO, USA). Nitrocellulose were then incubated with the corresponding anti-mouse or anti-rabbit IgG alkaline phosphatase-conjugated secondary antibodies (Sigma, St. Louis, MO, USA) for 1 hr at 37 °C at 1:1,000 or 1:30,000 dilution respectively. Blots were subsequently detected by incubating the membranes with nitro blue tetrazolium/5bromo-4-chloro-3-indolyl phosphate (NBT/BCIP, Roche). Optical density of the bands was evaluated using the Total Lab Quant software (Newcastle, England). Blots shown are representative of five independent experiments performed.

Immunoprecipitation

Cells prepared, as indicated for western blot, were also processed for immunoprecipitation in order to better clarify whether 3-nitro-L-tyrosine co-localized with α-tubulin. Cell lysates were washed with ice-cold PBS, and the insoluble materials were removed by centrifugation at 15,000 g for 40 min, and the supernatant (same amount of proteins) was incubated overnight at

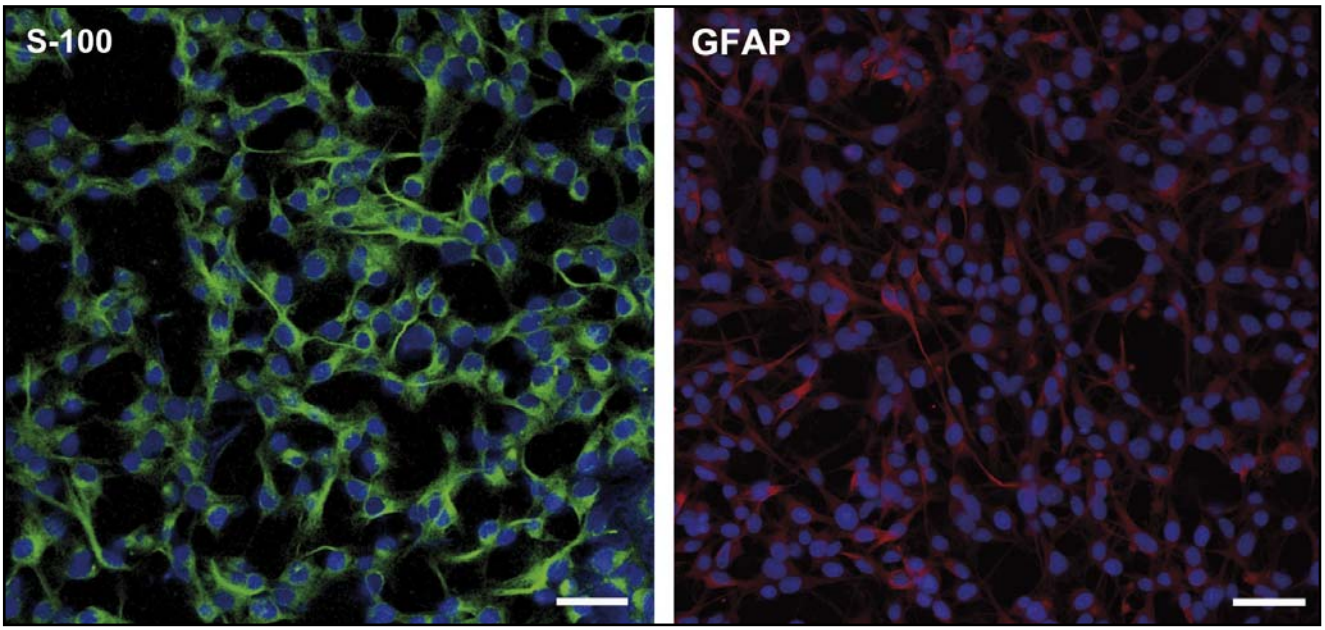

Fig. 1. Immunofluorescence staining. Ctrl cells were well stained with phenotypical Schwann cell marker S-100 and GFAP. Bar=50 µm

4 °C with 1 mg/mL anti-α tubulin monclonal antibody. The immunocomplexes were incubated with protein G-Sepharose (Protein G Immunoprecipitation kit, Sigma, St. Louis, MO, USA). The immunocomplexes immobilized on the protein G-Sepharose were sedimented by centrifugation at 10,000 g for 1 min, washed four times with the same lysis buffer, and resuspended in 50 reducing SDS sample buffers. The immunoprecipitated proteins were subjected to 10% SDS–PAGE under reducing conditions and electrophoretically transferred to nitrocellulose membranes then incubated overnight at 4 °C with anti 3-nitro-L-tyrosine polyclonal antibody (polyclonal, 1:500, Sigma, St. Louis, MO, USA). Nitrocellulose were then incubated with the corresponding anti-rabbit IgG alkaline phosphatase-conjugated antibody (Sigma, St. Louis, MO, USA). Blots were subsequently detected by incubating the membranes with nitro blue tetrazolium/5bromo-4-chloro-3-indolyl phosphate (NBT/BCIP, Roche). Optical density of the bands was evaluated using the Total Lab Quant software (Newcastle, England).

Indirect immunofluorescence staining of cell monolayers and confocal microscopy

The intracellular distributions of tubulin post-translational modifications and 3NT were further studied by indirect immunofluorescence staining. In order to perform single or double immunofluorescence, stained cells were seeded on 8 wells chamber slides (Lab-Tek, Naperville, ILL, USA). Scheduled times, medium characteristics, D-glucose concentrations, etc. were those indicated above. Cells were fixed in methanol at –20 °C and incubated overnight with antibodies against total α-tubulin (monoclonal, clone DM1A, 1:400, Sigma, St. Louis, MO, USA), tyrosinated α-tubulin (monoclonal, clone TUB-1A2, 1:400, Sigma, St. Louis, MO, USA), detyrosinated α-tubulin (polyclonal, 1:400, Chemicon-Millipore, USA), acetylated α-tubulin (monoclonal, clone 6-11B-1, 1:500, Sigma, St. Louis, MO, USA), 3-nitro-L-tyrosine (polyclonal, 1:500, Sigma, St. Louis, MO, USA). Secondary anti-rabbit and anti-mouse fluorescein/tetramethylrhodamine isothiocyanate-conjugated antibodies (FITC-AlexaFluor 488, TRITC-AlexaFluor 594, 1:400, Invitrogen, Carlsbad, CA, USA), were used. Additional monolayers were used as negative controls, by omitting the primary antibodies. All images were obtained with a confocal laser scanning microscope from Leica (TCS SP5 DMI 6000CS, Leica Microsystems GmbH, Wetzlar, Germany) using a 40/60× oil objective. FITC was exited at 488 nm and emission was detected between 510 and 550 nm. Rhodamine was excited at 568 nm and emission was detected between 585 and 640 nm. Nuclear counterstaining was performed using Hoescht blue-33342 (1:5,000, Sigma, St. Louis, MO, USA). Quantitative analysis of fluorescence intensity was performed using the Leica LAS AF Lite image analysis software package (Leica Microsystems GmbH, Wetzlar, Germany).

Statistical analysis

Average values used for analysis are representative of five experiments for each protocol. Data are expressed as mean ± standard error (SEM), and the inter-group analysis was done by Student's *t*-test or ANOVA. Statistical significance was accepted when $p<0.05$.

RESULTS

Morphological features

Observation under phase contrast optics revealed that Schwannoma cells treated with 180mM D-glucose (Gluc cells) displayed several morphological alterations, such as globular shape (white arrow), vacuols (black arrow), lack of characteristic cytoplasmic processes and were reduced in number,. This trend was increasingly evident from 24 to 72 hours, in comparison with control cells. Through the MTT proliferation assay, a significant reduction in the rate of cell growth was already evident at 48 hours after seeding, in the cells exposed to high glucose in comparison with controls (Figure 2).

Western blot analysis

Western blot analysis showed in glucose exposed cells (Gluc cells) a downregulation of total, tyrosinated and detyrosinated α-tubulin. Interestingly, a significant increase in acetylated α-tubulin in comparison with control cells was found (Figure 3). In order to evaluate the glucose-induced nitrosative-stress condition, we investigated the expression of 3-nitro-L-tyrosine, a widely recognized marker of nitrosative stress, and of catalase, one of the most abundant antioxidants. The antibody against 3-nitro-L-tyrosine revealed a higher amount of a single nitrated protein migrating a 55kDa in Gluc cells in comparison with control cells (Figure 4). The immunoprecipitation technique confirmed the co-localization of 3-nitro-L-tyrosine with α-tubulin (Figure 5). The antibody against catalase, showed a down-regulation in Gluc cells in comparison with controls (Figure 6). Western blot analysis of other cytoskeletal components such as actin and GFAP, did not reveal any differences in comparison with control cells (Figure 7). Furthermore,a decrease in Sirt2, the deacetylase enzyme, was detected in Gluc cells (Figure 8). Equal protein loading was ascertained by using a β-actin antibody; the β-actin levels did not change in the control and all the treated cells.From all blots obtained, a diagram was drawn in order to quantify the optical density of the bands.

Immunofluorescence staining

The results from immunofluorescence staining and confocal microscopy, confirm our data obtained by Western blot analysis. Indeed, a decreased immunoreactivity in total, tyrosinated and detyrosinated α-tubulin was seen in Gluc cells in comparison with controls. An increase in acetylated α-tubulin immunoreactivity was highly appreciable (Figures 9–10). Regarding the 3-nitro-L-

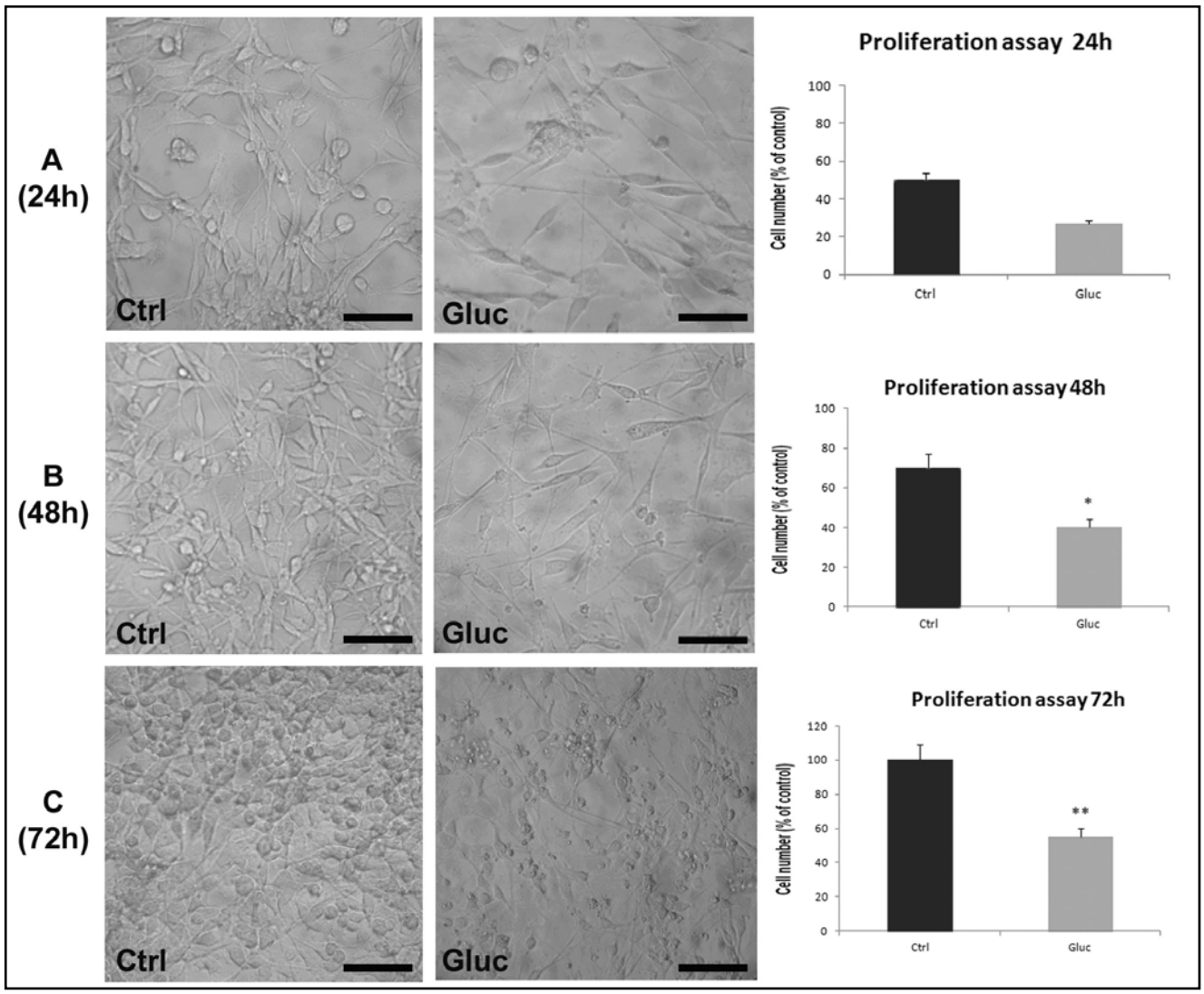

Fig. 2. Phase contrast optics and proliferation assay 180mM D-glucose-exposed cells (Gluc cells) are not confluent and display several morphological alterations, such as globular shape (black arrow) and vacuols (white arrow), in comparison with Ctrl. The trend of growth between Ctrl and Gluc cells is well appreciable in the diagrams of proliferation assay scheduled at 24-78-72 hours. Scale bar =30μm. Data are expressed as means ± SEM of five experiments. *indicates significant differences from Ctrl (p<0.02); ** indicates significant differences from Ctrl (p<0.01).

tyrosine expression, immunofluorescence staining confirmed the increase of 3-nitro-L-tyrosine in gluc cells, in comparison with controls. In addition, merging of the pictures obtained with the 3-nitro-L-tyrosine and α-tubulin antibodies showed a strong colocalization between 3-nitro-L-tyrosine and α-tubulin (Figure 11). Through confocal microscopy, morphological alterations in the distribution and the features of microtubular network in Gluc cells were more appreciable than with phaco examination (Figure 12).

DISCUSSION

Peripheral neuropathy is one of the major complications of the diabetic state. Prolonged hyperglycemic condition may induce changes in both axons and Schwann cells, and the latter seem to play a pivot role in the pathogenesis of metabolic neuropathies (Lehmann & Hoke 2010; Almhanna *et al.* 2002).

In the present study, rat Schwannoma cell line cultured under a high glucose condition revealed selective detrimental hyperglycemic effects on microtubular network. Western blot analysis and immunofluorescence staining indicate changes in the expression of the different post-translational α-tubulins investigated. Indeed, in D-glucose-exposed cells a decreased amount in total α-tubulin, tyrosinated α-tubulin and detyr α-tubulin and an increase in acetylated α-tubulin was observed. High D-glucose effects in total, tyrosinated and detyrosinated α-tubulin expression could be related to the presence of a high amount of 3-nitro-L-tyrosine revealed by Western blot analysis and immunofluores-

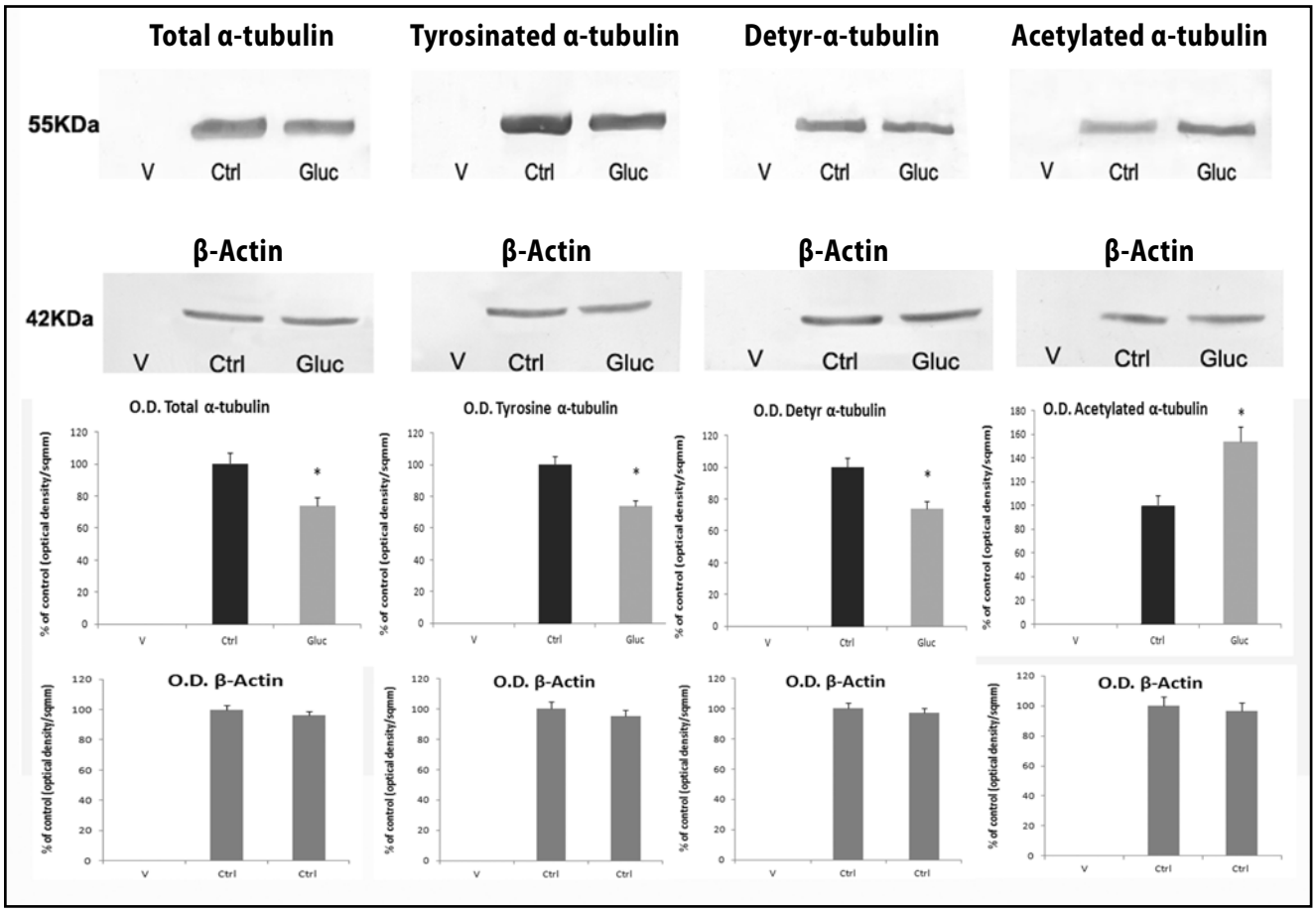

Fig. 3. Western blot of tubulins, shows a decrease in the amount of total, tyrosinated and detyrosinated alpha tubulin in Gluc cells. On the contrary, an increase of acetylated alpha tubulin amount in Gluc cells is well evident, in comparison with Ctrl cells. Data are confirmed by the diagram with the quantification of the intensity of each band. Data are expressed as means ± SEM of five experiments. * indicates significant differences from Ctrl ($p<0.02$).

cence. We know that in microtubules, one of the best investigated post-translational modifications is the reversible α-tubulin tyrosination cycle, through the removal and reincorporation of tyrosine at the carboxyl terminus by carboxypeptidase (CCP1) and tyrosine-tubulin ligase (TTL) respectively (Rosenbaum 2000; McRae *et al.* 1997). This posttranslational modification leads to two different α-tubulin isoforms: tyrosinated and detyrosinated. 3-nitro-L-tyrosine seems to be a good substrate for TTL (Kalisz *et al.* 2000) and can be selectively incorporated into detyrosinated α-tubulin and no other proteins, in an irreversible manner, since 3-nitro-L-tyrosine seems to be resistant to cleavage by CCP1. Indeed, once *nitrotyrosinated*, α-tubulin cannot be detyrosinated again (Chang *et al.* 2002; Kalisz *et al.* 2000; Eiserich *et al.* 1999), although this is still a matter of debate among other authors (Bisig *et al.* 2002). The nitrotyrosination of α-tubulin leads to microtubule malfunctions which may end with morphological alterations and apoptosis (Jovanović *et al.* 2010; Peluffo *et al.* 2004; Mihm *et al.* 2001; Nakazawa *et al.* 2000). The biological implications of 3-nitro-L-tyrosine could be at the basis of the morphological features observed in glucose-exposed cells. The continuous cell line used for our experiment, normally reaches 70–80% confluence within 48 hours from seeding, and this is the case of our Ctrl cells. On the contrary, cells exposed to glucose, after 48 hrs from seeding showed only about 40% of confluence and exhibit morphological changes (rounded shapes, loss of cytoplasmic processes, vacuols), well evident in the phase contrast at 72 hours from the seeding. These cell features corroborate the results of our preliminary work, where we found morphological, viability and proliferative changes in high-glucose exposed schwannoma cells, expressing high levels of 3-nitro-L-tyrosine (Gadau 2012). The incorporation of 3-nitro-L-tyrosine in the C terminus of α-tubulin could be at the basis of the progressive disruption of the normal architecture of microtubules as confirmed by our confocal microscopy results. Interestingly, the effect of oxidative stress induced by high glucose concentration, appears to selectively affect the microtubular network, since there were no significant changes in actin and the GFAP, suggesting no involvement of microfilaments in the negative effects of hyperglycaemia in Schwannoma cell line. Besides the presence of 3-nitro-L-tyrosine, in

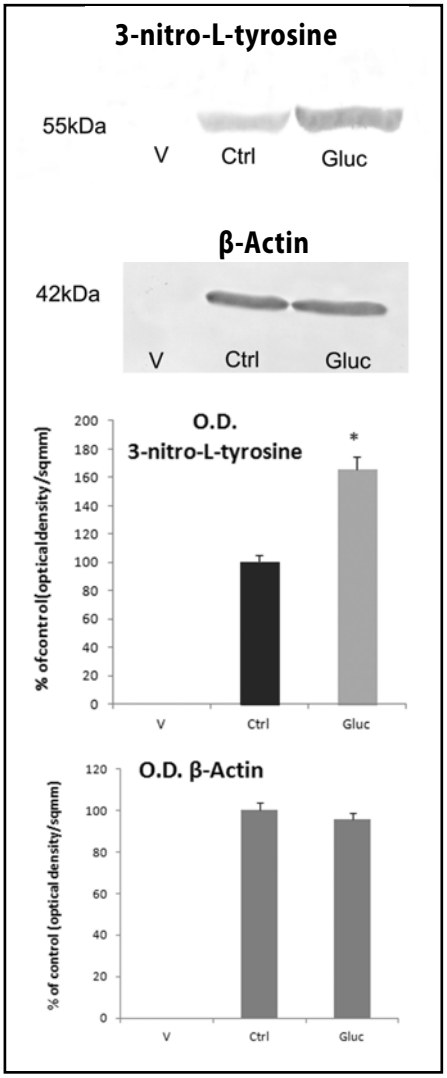

Fig. 4. Western blot of 3-nitro-L-tyrosine, shows an increase in the amount of the nitrated protein in Gluc cells. Data are confirmed by the diagram with the quantification of the intensity of each band. Data are expressed as means ± SEM of five experiments. * indicates significant differences from Ctrl (p<0.002).

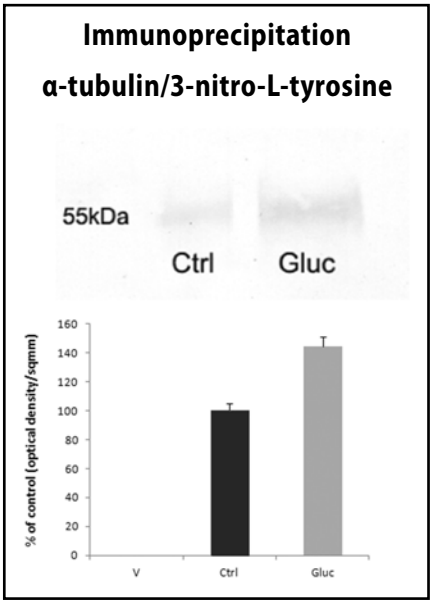

Fig. 5. Immunoprecipitation confirms the incorporation of 3-nitro-L-tyrosine into α tubulin. Data are confirmed by the diagram with the quantification of the intensity of each band. Data are expressed as means ± SEM of five experiments. * indicates significant differences from Ctrl (p<0.01).

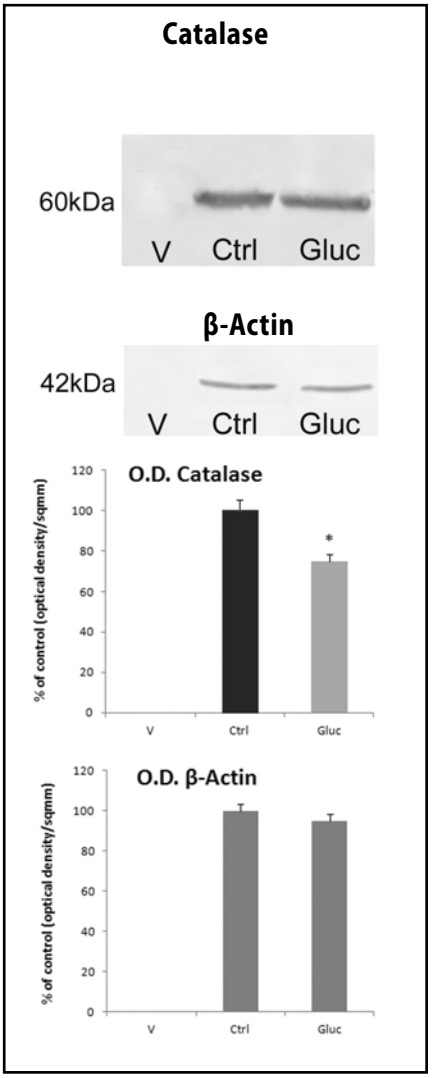

Fig. 6. Western blot of Catalase showed a reduced amount of the protein in Gluc cells in comparison with Ctrl. Data are confirmed by the diagram with the quantification of the intensity of bands. Data are expressed as means ± SEM of five experiments. * indicates significant differences from Ctrl (p<0.02).

our experiment, an oxidative/nitrosative stress condition high-glucose induced seems to be strengthened by the decreased amount displayed by catalase. Catalase is a well studied enzyme that plays a crucial role in protecting cells against toxic effects of hydrogen peroxide (Goyal & Basak 2010). Evidence reported that during oxidative stress condition, the high levels of RNS can overload the efficient detoxifying capability of cells leading to an inhibition of catalase antioxidant system (Baud *et al.* 2004; Liddell *et al.* 2004).

The hyperglycemic oxidative stress condition could also be linked to the increase of acetylated α-tubulin found, but in a different manner to the one described for the other tubulins. The acetylation/deacetylation cycle of α-tubulin could be mediated by two specific enzymes: a N-acetyltransferase for the acetylation and the deacetylases HDAC6 and Sirt2 (Perdiz *et al.* 2011; Harting & Knoll 2010; Zhao *et al.* 2010). Evidence reported that HDAC6 is highly expressed in neuronal cells, like Purkinje cells, whereas Sirt2 is mainly typical of glial cells such as oligodendrocyte and Schwann cells. Our attention was focused on Sirt2 expression, since our cells were glial type. Sirt2 is a member of a NAD-dependent histone deacetylases, localized almost exclusively in the cytoplasm, co-localizing with tubulin and able to remove the lysine-40 of tubulin (Tang & Chua 2008; Li *et al.* 2007; Southwood *et al.* 2007; North *et al.* 2003). Western blot results underlined a decrease in the amount of Sirt2, and this could be strictly related to the increase of α-tubulin acetylation found. The

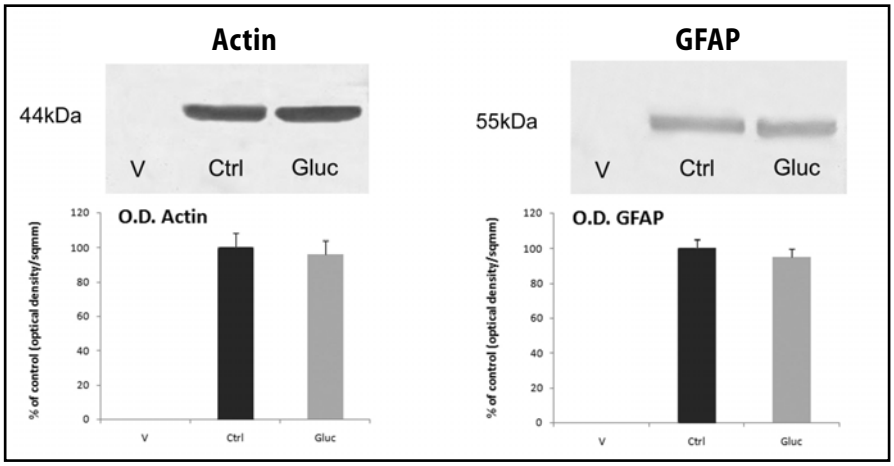

Fig. 7. Western blot of Actin and GFAP, shows no differences in the amount between Gluc and Ctrl cells Data are confirmed by the diagram with the quantification of the intensity of each band. Data are expressed as means ± SEM of five experiments.

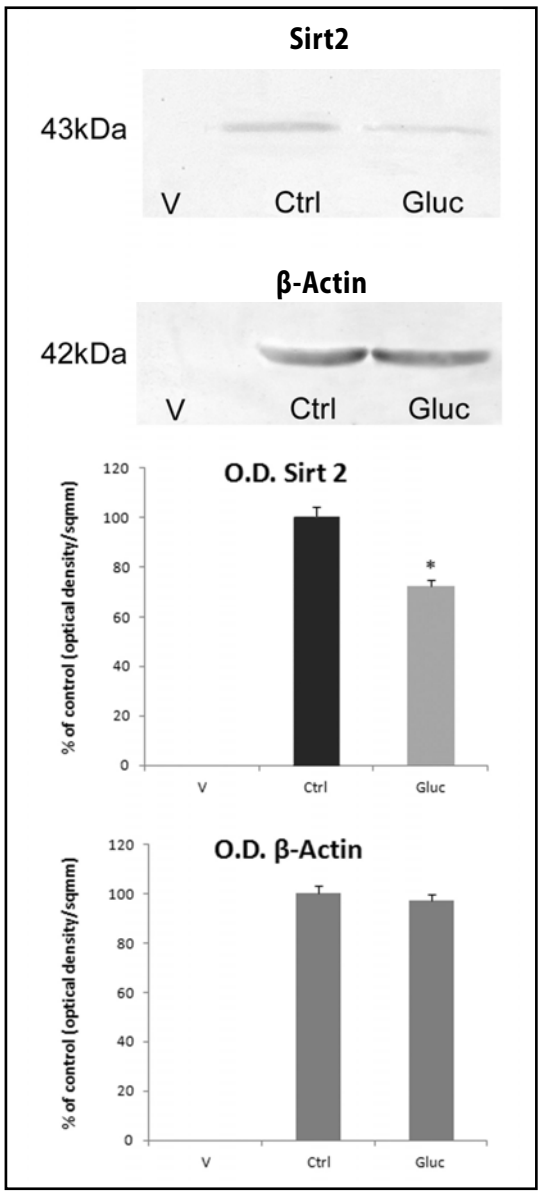

Fig. 8. Western blot of Sirt2, shows a decreased amount of the deacetylase in Gluc cells in comparison with Ctrl cells. Data are confirmed by the diagram with the quantification of the intensity of the bands. Data are expressed as means ± SEM of five experiments. *indicates significant differences from Ctrl (p<0.02).

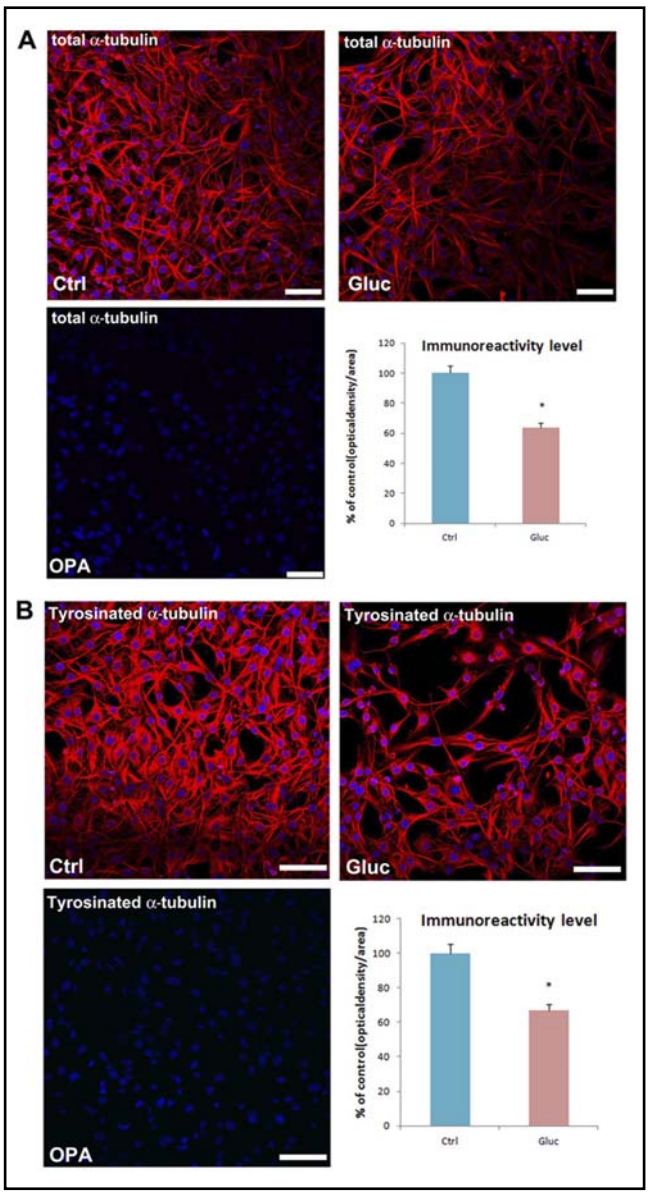

Fig. 9. Immunofluorescence staining. Labelling with anti total and tyrosine alpha tubulin antibodies, shows less staining immunoreactivity in Gluc cells in comparison with Ctrl. The diagram on the right quantifies the immunoreactivity level of the cells. Data are expressed as means ± SEM of five experiments. * indicates significant differences from Ctrl (p<0.02). OPA= omission primary antibody. Bar=50 µm.

high-glucose nitrosative induced condition could be at the basis of the Sirt2 downregulation. Indeed, in some pathological conditions, the oxidative stress status could suppress Sirt2 expression, leading to alteration of cytoskeleton structures through an increase of tubulin acetylation (Wu *et al.* 2010). However, the involvement of tubulin hyperacetylation on Schwannoma cellular modifications is less clear despite the role played by the nitrotyrosination of tubulin. Indeed, there are conflicting theories about the disturbance of the increased α-tubulin acetylation in the pathogenesis or in the rescue of certain neural disorders (Dompierre *et al.* 2007; Outeiro *et al.* 2007). As regards the role played by α-tubulin hyperacetylation in our experiment, one possible explanation could be related to the fact that Sirt2 usually increases during the M phase of the cell cycle, regulating critical phases of cellular mitosis (Dryden *et al.* 2003). Evidence reported that in experimental conditions, an hinibition of deacetylases improves the rate of acetylation of tubulin, creating very stable microtu-

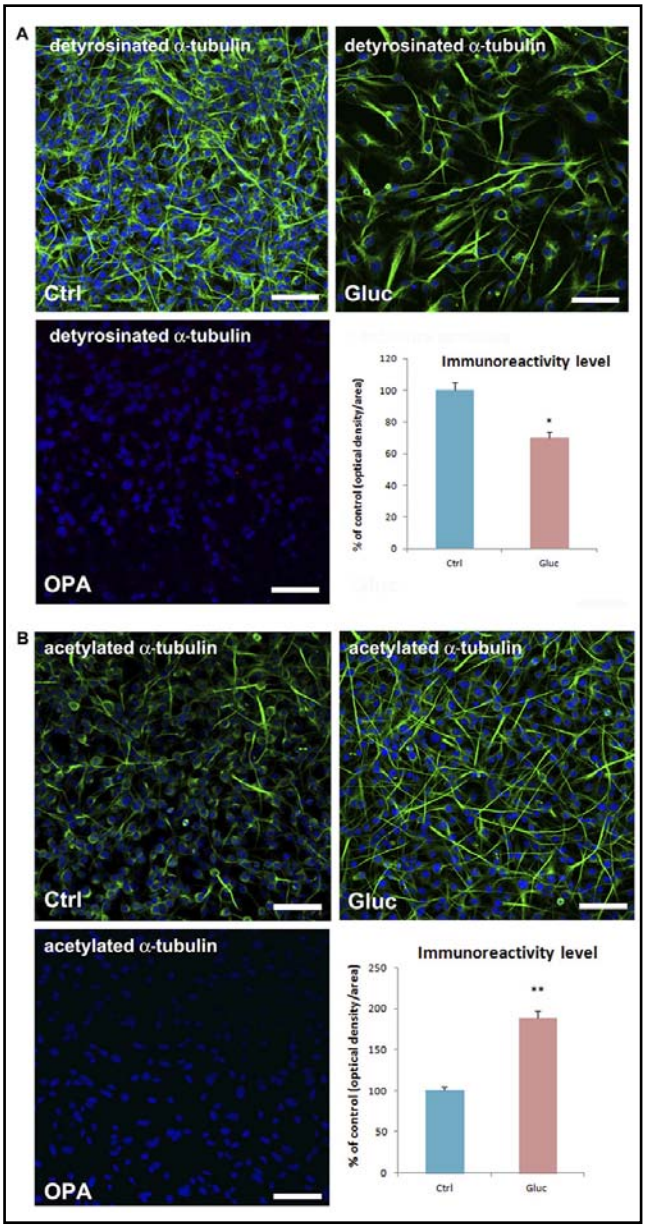

Fig. 10 (left). Immunofluorescence staining. Labelling with anti detyr and acetylated alpha tubulin antibodies, shows less staining immunoreactivity in Gluc cells in comparison with Ctrl as regards detyr alpha tubulin. In contrast a strong immunoreactivity for acetylated alpha tubulin is well evident in Gluc cells in comparison with control. The diagram quantifies the immunoreactivity level of the cells. Data are expressed as means ± SEM of five experiments. * indicates significant differences from Ctrl (p<0.02); ** indicates significant differences from Ctrl (p<0.001). OPA= omission primary antibody. Bar=50 µm.

Fig. 11 (below). Double fluorescence staining with anti total alpha tubulin and 3-nitro-L-tyrosine antibodies. The fluorescence shows an increase of 3-nitro-L-tyrosine immunoreactivity in Gluc cells in comparison with Ctrl. Moreover, good overlapping is well detectable in the merge pics, between the two proteins, indicating a co-localization of 3-nitro-L-tyrosine with total alpha tubulin. In Gluc cells a prevalence of the nitrated protein is evident. OPA= omission primary antibody. Bar=50 µm.

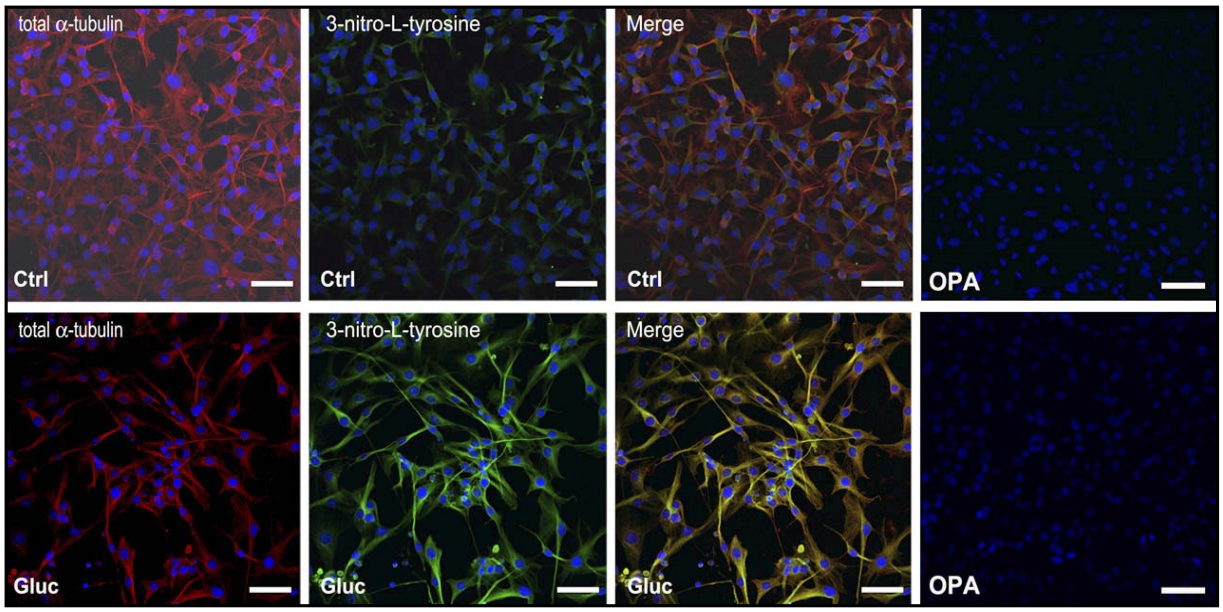

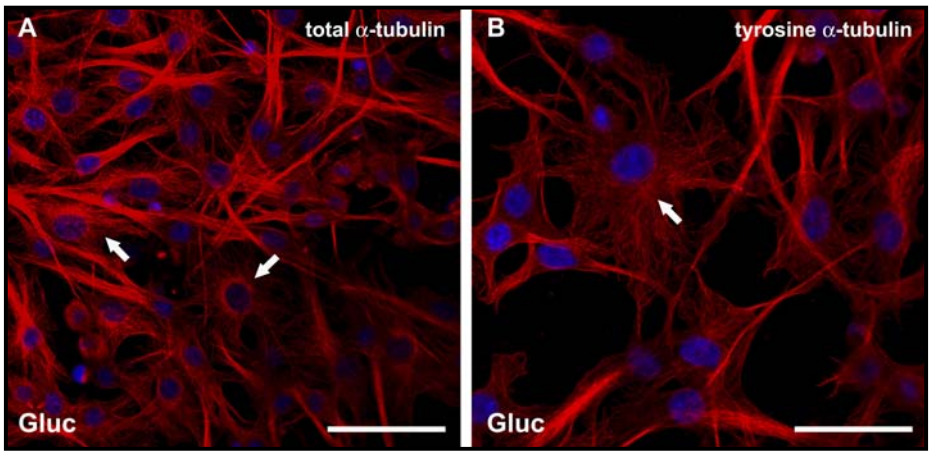

Fig. 12. Morphological alterations. Fluorescence staining to total and tyrosine α-tubulin of Gluc cells, showed noticeable changes (white arrow) in the normal structure of the microtubular network, with subsequent severe cell shape alterations. Bar=50 μm.

bules, with subsequent alteration of spindle microtubule dynamics that may block mitosis and facilitate cell death (Lawson *et al.* 2010; Catalano *et al.* 2007).

To sum up, our results underline the importance of nitrosative-induced microtubular alterations in the PNS, during hyperglycemic conditions. This supports the results of our previous work, suggesting that microtubular network may be considered a target for the ROS generated under hyperglicaemic conditions (Gadau *et al.* 2009; Gadau *et al.* 2008). Our data may suggest that Schwann cells, which are often "neglected" because of their supporting role to their more "glamourous" cousins, neurons, might be directly involved in the pathogenesis of diabetic neuropathy, through the impairment of their microtubular network.

AKNOWLEDGMENTS

This work was supported by funds from the Sardinia Region, Regional Law 7-CRP-25879/2011.

REFERENCES

1 Akella AJ, Wloga D, Kim J, Starostina NG, Lyons-Abbott S, Morrissette NS, Dougan ST, Kipreos ET, Gaertig J (2010). MEC-17 is an alpha-tubulin acetyltransferase. Nature. **467**: 218–222.
2 Allani PK, Sum T, Bhansali SG, Mukherjee SK, Sonee M (2004). A comparative study of the effect of oxidative stress on the cytoskeleton in human cortical neurons. Toxicol Appl Pharmacol. **196:** 29–36.
3 Almhanna K, Wilkins PL, Bavis JR, Harwalkar S, Berti-Mattera LN (2002). Hyperglycemia triggers abnormal signaling and proliferative responses in Schwann cells. Neurochem Res. **27**: 1341–1347.
4 Baud O, Greene AE, Li J, Wang H, Volpe JJ, Rosenberg PA (2004). Glutathione peroxidase-catalase cooperativity is required for resistance to hydrogen peroxide by mature rat oligodendrocytes. J Neurosci **24**: 1531–1540.
5 Baynes JW, Thorpe SR (1999). Role of oxidative stress in diabetic complications: a new perspective on an old paradigm. Diabetes **48**: 1–9.
6 Bellomo G and Mirabelli F (1992). Oxidative stress and cytoskeletal alterations. Ann N Y Acad Sci. **663**: 97–109.
7 Bisig CG, Purro SA, Contín MA, Barra HS, Arce CA (2002). Incorporation of 3-nitrotyrosine into the C-terminus of alpha-tubulin is reversible and not detrimental to dividing cells. Eur J Biochem. **269**: 5037–5045.
8 Blanchard-Fillion B, Prou D, Polydoro M, Spielberg D, Tsika E, Wang Z, et al (2006). Metabolism of 3-nitrotyrosine induces apoptotic death in dopaminergic cells. J Neurosci. **26:** 6124–6130.
9 Bloom K (2004). Microtubule composition: cryptography of dynamic polymers. Proc Natl Acad Sci U S A. **10:** 6839–6840.
10 Boyault C, Sadoul K, Pabion M, Khochbin S (2007). HDAC6, at the crossroads between cytoskeleton and cell signaling by acetylation and ubiquitination. Oncogene. **26**: 5468–5476.
11 Brownlee M (2001). Biochemistry and molecular cell biology of diabetic complications. Nature **414:** 813–820.
12 Catalano MG, Poli R, Pugliese M, Fortunati N, Boccuzzi G (2007). Valproic acid enhances tubulin acetylation and apoptotic activity of paclitaxel on anaplastic thyroid cancer cell lines. Endocr Relat Cancer. **14**: 839–845.
13 Chang W, Webster DR, Salam AA, Gruber D, Prasad A, Eiserich JP, Bulinski JC (2002). Alteration of the C-terminal amino acid of tubulin specifically inhibits myogenic differentiation. J Biol Chem. **277**: 30690–30698.
14 Cheng C, Zochodne DW (2003). Sensory neurons with activated caspase-3 survive long-term experimental diabetes. Diabetes. **52**: 2363–2371.
15 Delaney CL, Russell JW, Cheng HL, Feldman EL (2001). Insulin-like growth factor-I and over-expression of Bcl-xL prevent glucose-mediated apoptosis in Schwann cells. J Neuropathol Exp Neurol. **60**: 147–160.
16 Dompierre JP, Godin JD, Charrin BC, Cordelieres FP, King SJ, Humbert S, Saudou F (2007). Histone deacetylase 6 inhibition compensates for the transport deficit in Huntington's disease by increasing tubulin acetylation. J Neurosci. **27**: 3571–3583.
17 Dryden SC, Nahhas FA, Nowak JE, Goustin AS, Tainsky MA (2003). Role for human SIRT2 NAD-dependent deacetylase activity in control of mitotic exit in the cell cycle. Mol Cell Biol. **23**: 3173–3185.
18 Drel VR, Pacher P, Stevens MJ, Obrosova IG (2006). Aldose reductase inhibition counteracts nitrosative stress and poly(ADP-ribose) polymerase activation in diabetic rat kidney and high-glucose-exposed human mesangial cells. Free Radic Biol Med. **40**: 1454–1465.
19 Eiserich JP, Estevez AG, Bamberg TV, Ye YZ, Chumley PH, Beckman JS, Freeman BA (1999). Microtubule dysfunction by post-translational nitrotyrosination of alpha-tubulin: a nitric oxide-dependent mechanism of cellular injury. Proc Natl Acad Sci USA. **96**: 6365–6370.

20 Ersfeld K, Wehland J, Plessmann U, Dodemont H, Gerke V, Weber K (1993). Characterization of the tubulin-tyrosine ligase. J Cell Biol. **120**: 725–732.
21 Feldman EL (2003). Oxidative stress and diabetic neuropathy: a new understanding of an old problem. J Clin Invest. **111**: 431–433.
22 Finkel T (2003). Oxidant signals and oxidative stress. Curr Opin Cell Biol. **15**: 247–54.
23 Fukushima N, Furuta D, Hidaka Y, Moriyama R, Tsujiuchi T (2009). Post-translational modifications of tubulin in the nervous system. J Neurochem. **109**: 683–693.
24 Gadau SD (2012). Nitrosative stress induces proliferation and viability changes in high glucose-exposed rat Schwannoma cells. Neuroendocrinol Lett. **33**: 279–284.
25 Gadau S, Lepore G, Zedda M, Mura A, Farina V (2009). Different nitrosative-induced microtubular modifications and testosterone neuroprotective effects on high-D-glucose-exposed neuroblastoma and glioma cells. Neuroendocrinol Lett. **30**: 515–524.
26 Gadau S, Lepore G, Zedda M, Manca P, Chisu V, Farina V (2008). D-Glucose induces microtubular changes in a neural cell line through the incorporation of 3-nitro-L-tyrosine into tubulin. Arch It Biol. **146**: 107–117.
27 Goyal MM, Basak A (2010). Human catalase: looking for complete identity. Protein Cell. **1:** 888–897.
28 Hai M, Muja N, DeVries GH, Quarles RH, Patel PI (2002). Comparative analysis of Schwann cell lines as model systems for myelin gene transcription studies. J Neurosci Res. **69**: 497–508.
29 Halliwell B (2006). Oxidative stress and neurodegeneration: where are we now? J Histochem. **97**: 1634–1658.
30 Halliwell B (2001). Role of free radicals in the neurodegenerative diseases: therapeutic implications for antioxidant treatment. Drugs Aging. **18**: 685–716.
31 Hammond JW, Cai D, Verhey KJ (2008). Tubulin modifications and their cellular functions. Curr Opin Cell Biol. **20**: 71–76.
32 Harting K, Knöll B (2010). SIRT2-mediated protein deacetylation: An emerging key regulator in brain physiology and pathology. Eur J Cell Biol. **89**: 262–269.
33 Hattangady NG, Rajadhyaksha MS (2009). A brief review of in vitro models of diabetic neuropathy. Int J Diabetes Dev Ctries. **29**: 143–149.
34 Janke C, Kneussel M (2010). Tubulin post-translational modifications: encoding functions on the neuronal microtubule cytoskeleton. Trends Neurosci. **33**: 362–372.
35 Jovanović, AM, Durst S, Nick P (2010). Plant cell division is specifically affected by nitrotyrosine. J Exp Bot. **61**: 901–909.
36 Kalisz HM, Erck C, Plessmann U, Wehland J (2000). Incorporation of nitrotyrosine into alpha-tubulin by recombinant mammalian tubulin-tyrosine ligase. Biochim Biophys Acta. **1481**: 131–138.
37 Ishii N, Patel KP, Lane PH, Taylor T, Bian K, Murad F, et al (2001). Nitric oxide synthesis and oxidative stress in the renal cortex of rats with diabetes mellitus. J Am Soc Nephrol. **12**: 1630–1639.
38 Lawson M, Uciechowska U, Schemies J, Rumpf T, Jung M, Sippl W (2010). Inhibitors to understand molecular mechanisms of NAD(+)-dependent deacetylases (sirtuins). Biochim Biophys Acta. **1799**: 726–739.
39 Lehmann HC, Höke A (2010). Schwann cells as a therapeutic target for peripheral neuropathies. CNS Neurol Disord Drug Targets. **9**: 801–806.
40 Li W, Zhang B, Tang J, Cao Q, Wu Y, Wu C, et al (2007). Sirtuin 2, a mammalian homolog of yeast silent information regulator-2 longevity regulator, is an oligodendroglial protein that decelerates cell differentiation through deacetylating alpha-tubulin. J Neurosci. **27**: 2606–2616.
41 Liddell JR, Robinson SR, Dringen R (2004). Endogenous glutathione and catalase protect cultured rat astrocytes from the iron-mediated toxicity of hydrogen peroxide. Neurosci Lett. **364**: 164–167.
42 MacRae TH (1997). Tubulin post-translational modifications. Enzymes and their mechanisms of action. Eur J Biochem. **244**: 265–278.
43 Melo A, Monteiro L, Lima RM, Oliveira DM, Cerqueira MD, El-Bachá RS (2011). Oxidative stress in neurodegenerative diseases: mechanisms and therapeutic perspectives. Oxid Med Cell Longev. **467180**: 1–14.
44 Mihm MJ, Schanbacher BL, Wallace BL, Wallace LJ, Uretsky NJ, Bauer JA (2001). Free 3-nitrotyrosine causes striatal neurodegeneration in vivo. J Neurosci. **21**: 1–5.
45 Nakazawa H, Fukuyama N, Takizawa S, Tsuji C, Yoshitake M, Ishida H (2000). Nitrotyrosine formation and its role in various pathological conditions. Free Radic Res. **33:** 771–784.
46 North BJ, Marshall BL, Borra MT, Denu JM, Verdin E (2003). The human Sir2 ortholog, SIRT2, is an NAD+-dependent tubulin deacetylase. Mol Cell. **11**: 437–444.
47 Outeiro TF, Kontopoulos E, Altmann SM, Kufareva I, Strathearn KE, Amore AM, et al (2007). Sirtuin 2 inhibitors rescue alpha-synuclein-mediated toxicity in models of Parkinson's disease. Science. **317**: 516–519.
48 Pacher P, Obrosova IG, Mabley JG., Szabó C (2005). Role of nitrosative stress and peroxynitrite in the pathogenesis of diabetic complications. Emerging new therapeutical strategies. Curr Med Chem. **12**: 267–275.
49 Peluffo H, Shacka JJ, Ricart K, Bisig CG, Martinez-Palma L, Pritsch O, et al (2004). Induction of motor neuron apoptosis by free 3-nitro-L-tyrosine. J Neurochem. **89**: 602–612.
50 Pennathur S, Heinecke JW (2004). Mechanisms of oxidative stress in diabetes: implications for the pathogenesis of vascular disease and antioxidant therapy. Front Biosci. **9**: 565–574.
51 Perdiz D, Mackeh R, Poüs C, Baillet A (2011). The ins and outs of tubulin acetylation: more than just a post-translational modification? Cell Signal. **23**: 763–771.
52 Rogers KR, Morris CJ, Blake DR (1989). Cytoskeletal rearrangement by oxidative stress. Int J Tissue React. **11**: 309–314.
53 Rosenbaum J (2000). Cytoskeleton: functions for tubulin modifications at last. Curr Biol. **10**: 801–803.
54 Sarchielli P, Galli F, Floridi A, Floridi A, Gallai V (2003). Relevance of protein nitration in brain injury: a key pathophysiological mechanism in neurodegenerative, autoimmune, or inflammatory CNS diseases and stroke. Amino Acids. **25**: 427–436.
55 Sayre LM, Perry G, Smith MA (2008). Oxidative stress and neurotoxicity. Chem Res Toxicol. **21**: 172–188.
56 Southwood CM, Peppi M, Dryden S, Tainsky MA, Gow A (2007). Microtubule deacetylases, SirT2 and HDAC6, in the nervous system. Neurochem Res. **32**: 187–195.
57 Tang BL, Chua CE (2008). SIRT2, tubulin deacetylation, and oligodendroglia differentiation. Cell Motil Cytoskeleton. **65**: 179–182.
58 Therond P (2006). Oxidative stress and damages to biomolecules (lipids, proteins, DNA). Ann Pharm Fr. **64**: 383–389.
59 Thuraisingham RC, Nott CA, Dodd SM, Yaqoob MM (2000). Increased nitrotyrosine staining in kidneys from patients with diabetic nephropathy. Kidney Int. **57**: 1968–1972.
60 Vincent AM, Kato K, McLean LL, Soules ME, Feldman, EL (2009). Sensory neurons and schwann cells respond to oxidative stress by increasing antioxidant defense mechanisms. Antioxid Redox Signal. **11**: 425–438.
61 Wade RH (2009). On and around microtubules: an overview. Mol Biotechnol. **43**: 177–191.
62 Westermann S, Weber K (2003). Post-translational modifications regulate microtubule function. Nat Rev Mol Cell Biol. **4:** 938–947.
63 Wloga D, Gaertig J (2010). Post-translational modifications of microtubules. J Cell Sci. **123**: 3447–55.
64 Wu YT, Wu SB, Lee WY, Wei YH (2010). Mitochondrial respiratory dysfunction-elicited oxidative stress and posttranslational protein modification in mitochondrial diseases**.** Ann NY Acad Sci. **1201**: 3447–3455.
65 Yasuda H, Terada M, Maeda K, Kogawa S, Sanada M, Haneda M, Kashiwagi A, Kikkawa R (2003). Diabetic neuropathy and nerve regeneration. Prog Neurobiol. **69**: 229–285.
66 Zhao Z, Xu H, Gong W (2010). Histone deacetylase 6 (HDAC6) is an independent deacetylase for alpha-tubulin. Protein Pept Lett. **17**: 555–558.